Direct Plasmadynamic Conversion of Plasma Thermal Power to Electricity

Robert M. Mayo, *Member, IEEE*, and Randell L. Mills

***Abstract*—The generation of electrical energy using direct plasmadynamic conversion (PDC) is studied experimentally for small-scale, chemically-assisted plasmas (CA-plasma) for the first time. Glow discharge and microwave-generated plasma sources are operated at power levels on the order of a few to 50 W in the discharge case and up to 12.83 W/cm^3 in the microwave case. Extracted power approaching 1/4 W has been achieved as a demonstration. It is envisioned that such a system may be readily scaled to a few hundred Watts to several tens of kilowatts output power for microdistributed commercial applications (e.g., household, automotive, light industry, and space based power). Three-quarter inch long by 0.040-in diameter cylindrical PDC electrodes have been tested in a 10–50 W direct current, glow discharge plasma device with He or Ar as the working gas at 0.3–3.0 torr. The PDC anode was magnetized in the range of 0–700 G with a 1.5-in water cooled Helmholtz electromagnet. Open circuit voltages up to 6.5 V were obtained across the PDC electrodes at 1 torr He and 350-G field. The collector voltage was shown to be a function of applied magnetic field strength B and peaking at about 300 G. A variety of resistive loads were connected across the PDC electrodes, extracting continuous electrical power up to 0.44 mW. The power/load curve peaks at 0.44 mW for a 20 kΩ load indicating the impedance matching condition with the plasma source. The most severe limitation to collector output performance is shown to be plasma conductivity. Collector power drops sharply with increasing neutral gas fill pressure in the glow discharge chamber at constant discharge current indicating that electron collisions with neutral gas atoms are responsible for the reduction in conductivity. Scale-up to higher power has been achieved with the use of a microwave plasma generator. A 0.75-in long by 0.094-in diameter PDC anode was magnetized to $\sim$140 G resulting in open circuit PDC voltages in excess of 11.5 V for He plasmas at $\sim$0.75–1 torr and 50 sccm flow. Due to higher conductivity, load matching was now obtained at $\sim$600 Ω. Langmuir probe results indicate good agreement between the conductivity change and the electron to neutral density ratio scale-up. For this source and electrode configuration, PDC power as high as $\sim$200 mW was demonstrated in He at 0.75 torr for a microwave input power density of $\sim$8.55 W/cm^3. Considering an electron mean-free path as the scale for collector probe influence in the plasma, the peak extracted power density is $\sim$1.61 W/cm^3, corresponding to a volumetric conversion efficiency of $\sim$18.8%.**

***Index Terms*—Microwave plasma, plasmadynamic, power conversion.**

I. Introduction

HIGH-TEMPERATURE plasmas possess a substantial inventory of energy stored in the thermal and/or kinetic components of plasma ions, electrons, and, in some cases, neutral gas particles in some weakly ionized plasmas. There is obvious incentive in devising methods and technologies to efficiently extract this energy and convert it to a more useful form. Most often, conversion to electrical energy is desired as this form is readily stored and transmitted, and is efficiently converted to mechanical work at the delivery site.

A number of plasma energy conversion schemes have been studied in the four plus decades of controlled thermonuclear fusion research. At high temperature (as that produced in the blanket material of a high-power D-T fusion reactor) a thermal steam cycle [1], [2] is usually considered the most practical energy extraction means as the bulk (80%) of the energy release is in the form of chargeless neutrons. Thermal steam cycles are robust, reliable, proven technologies, and are well established as the work horse of modern electrical power delivery. Yet, the conversion efficiency is limited and high coolant temperatures are required. Furthermore, costs are prohibitive for the use of steam cycles in small, distributed power sources.

Direct conversion of plasma-charged particle kinetic to electric energy [3] may represent an attractive alternative to the steam cycle for at least several plasma systems of great interest including 1) the D-T fusion reactor (as a "topping" unit to extract the 20% of fusion energy in high energy charged particles), 2) advanced, a-neutronic fueled fusion reactors, and 3) chemically assisted (CA)-plasma cells [4]–[6]. In fusion reactors, the fully ionized, high-temperature (up to 10–15 keV) plasma energy may be readily extracted by direct, electrostatic means, thereby converting charged-particle kinetic energy to electrostatic potential energy via decelerating electrodes [3]. Whereas for CA-plasma cell devices, possessing only weakly ionized and relatively cold plasmas, conversion methods more compatible with a fluid environment like MHD converters [7] may be required to extract stored energy.

Herein, we demonstrate the plasmadynamic conversion (PDC) of plasma thermal to electrical energy from discharge and microwave plasmas as a illustration of power extraction from CA-plasma cells. As in MHD conversion, PDC extracts stored plasma energy directly. Unlike MHD, however, PDC does not require plasma flow. Instead, power extraction by PDC exploits the potential difference established between a magnetized and an unmagnetized electrode [8] immersed in a plasma to drive current in an external load and, thereby extract electrical power directly from the stored plasma thermal energy. For the first time, a substantial quantity of electrical power is extracted (up to 0.4 mW in the discharge plasma case and up to 220 mW in the microwave case). This scale-up is concomitant with a like increase in the plasma to neutral density ratio. Further power scale-up to commercially appropriate power

Manuscript received March 26, 2002; revised July 15, 2002.

The authors are with BlackLight Power, Inc., Cranbury, NJ 08512 USA (e-mail: rmayo@blacklightpower.com).

Digital Object Identifier 10.1109/TPS.2002.807496

levels is now realizable. The engineering relationships learned from these initial scoping studies can be applied to converting the thermal power from CA-plasmas to electrical power.

II. Theory

When an isolated (floating) conductor is inserted into a thermal plasma, it is predicted to attain the potential

$$V_f = V_p - \left[\frac{1}{2}\ln\left(\frac{2M}{\pi m}\right)\right]\frac{kT_e}{e} \tag{1}$$

referred to as the floating potential, by the steady, one-dimensional electron equation of motion (EOM) fixed ions unimpeded by the sheath potential. Here, V_p is the plasma potential, kT_e is the electron temperature, and M and m are the ion and electron masses, respectively. In the presence of a magnetic field of intermediate strength (i.e., sufficient to magnetize electrons but not ions) and parallel to the surface of the conductor, electron collection at the conductor is substantially reduced and the local floating potential is altered. While a complete and general description is rather involved, sufficient insight into the influence of magnetization can be gained by examining the collection of electron current near the space (plasma) potential [9]. This approach is justified since the impediment of electron current to a floating probe results in a modified floating potential, V_{fm}, such that $V_f < V_{fm} < V_p$ and approaching V_p. As magnetization (B) is provided only completely parallel to the probe surface facing the plasma, we consider only diffusive transport of electrons to the probe. In contrast to the situation described by (1), collisions are now required to allow an electron current to the probe. Current continuity [9] dictates that the electron density within one mean collision distance to the probe n' is given by

$$n' = \frac{n_o}{1+\beta}$$

with

$$\beta = \frac{A_p\overline{v}}{\pi CD}\,(1+\Omega^2)^{1/2}$$

where n_o is the plasma electron density far from the probe in the bulk plasma, A_p is the probe surface area, $\overline{v}$ is the average electron speed, C is the probe capacitance with respect to the surface at infinity with charge density n_o (taken to be at the plasma-sheath boundary), D is the mass diffusivity in the absence of B, Ω is the electron magnetization parameter ($\Omega = eB/m\nu_{en}$), and ν_{en} is the electron–neutral particle collision frequency. Only electron–neutral collisions need to be considered as neutral particles by far dominate the scattering interactions with electrons as the pressures considered here.

Since the probe is aligned parallel to B, the effective collision distance becomes the electron gyro-radius, r_L. Since x_s (sheath thickness) $\ll r_L \ll \lambda$ (mean free path), collisions may be ignored in the last gyro-step to the probe so that the Boltzmann relation applies

$$n = n'\exp\left[\frac{e}{kT_e}\,(V - V_p)\right]. \tag{2}$$

Balancing electron and ion currents, then, for the magnetized floating probe yields

$$V_{fm} = V_p - \frac{kT_e}{2e}\ln\left(\frac{2M}{\pi m}\right) + \frac{kT_e}{e}\ln(1+\beta). \tag{3}$$

This expression now replaces (1) in the magnetized as well as unmagnetized case ($B = 0$) since $\beta_o = \beta(\Omega = 0) \neq 0$ to include the effect of collisions on electron current in the limit $B \to 0$.

The PDC of thermal plasma energy to electricity is achieved by inserting two floating conductors in a plasma, one magnetized, the other unmagnetized. The potential difference between the two conductors (now appropriately referred to as electrodes) is given by the difference in unmagnetized and magnetized floating potential as described by (3) with β_o and β, respectfully. Referring to this potential difference as the open circuit PDC voltage, V_o, we have

$$V_o = \frac{kT_e}{e}\ln\left(\frac{1+\beta}{1+\beta_o}\right).$$

Since β and $\beta_o \gg 1$, the probe area and capacitance no longer enter the PDC voltage expression, so that

$$V_o = \frac{kT_e}{2e}\ln(1+\Omega^2). \tag{4}$$

In a strongly magnetized plasma ($\Omega \sim 20$) at 2 eV, a respectable $V_o \sim 6$ V can be expected. The $\ln B$ dependence at large B is expected from the Boltzmann relation [(2)] as the electron density reaching the probe decreases as $1/B$ for large field strength. It should be noted here that, in general, the conditions at the magnetized and unmagnetized probe may be different so that even when β and $\beta_o \gg 1$, the logarithmic term in (4) may retain the dependencies

$$\frac{\beta}{\beta_o} = \frac{A_p}{A_{p_o}}\,\frac{\overline{v}}{\overline{v}_o}\,\frac{C_o}{C}\,\frac{D_o}{D}\,(1+\Omega^2)^{1/2}$$

where the subscript "o" refers to conditions at the unmagnetized electrode. Increasing the magnetized electrode area or electron thermal speed at the electrode should incur increased PDC voltage, while the same should be expected with a reduction in effective probe capacitance or mass diffusivity near the probe. Modification to the probe surface area though is often the parameter in the most readily controlled by the experimenter. In addition, electrostatic potential difference generated by thermal gradients in the plasma have been neglected here. Placing the electrodes in regions of the plasma at different temperatures can further increase the collection potential [10].

Shorting the PDC electrodes with the load, R_L, allows the circuit to be completed, and current and power flow to the external load. The PDC source is necessarily loaded by this action, thereby reducing the source voltage to $V_o - iR$, where R is the internal resistance of the source (i.e., plasma and PDC electrode system). Assigning the loaded PDC voltage as

$$V_{\rm PDC} = V_o - iR$$

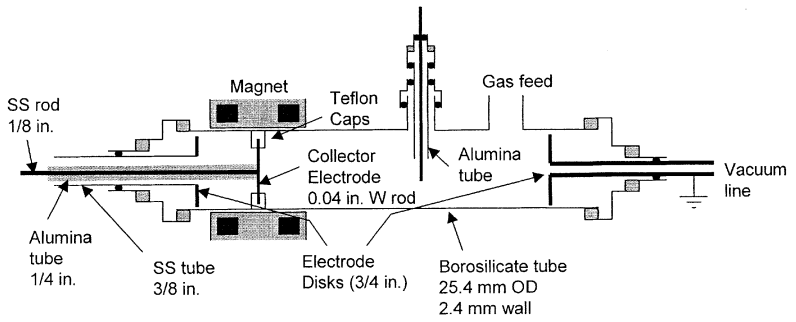

Fig. 1. Schematic of the 1-in glow-type discharge tube and PDC electrode assembly. The outer 0.75-in disk electrodes are the glow discharge electrodes. The magnetized PDC electrode is shown as the collector electrode. The unmagnetized PDC electrode is shown inside the vertical alumina tube.

where $i = V_o/(R + R_L)$, the extracted power is found

$$P_{\rm PDC} = \frac{R_L}{(R+R_L)^2}\, V_o^2.$$

As expected, the impedance matching condition $R = R_L$ determines the peak extracted power

$$P_{\max} = \frac{1}{4R_L}\, V_o^2. \tag{5}$$

In the $V_o \sim 6$ V example introduced earlier and with $R_L \sim 10$ kΩ, a maximum extracted power of 0.9 mW can be realized. Attaining 1 W of extracted power from PDC under these plasma conditions requires a source impedance matched to the load at $R_L \sim 9\ \Omega$.

III. Experimental Apparatus

Two separate PDC experiments are described here. In the first, a dc glow-type discharge plasma was generated in a 1-in diameter (OD) by 12-in glass tube. In the second, a 1.5-kW maximum output power microwave generator was used to generate plasma in a quartz applicator tube of similar dimensions. In both experiments, one magnetized (anode) PDC electrode and one unmagnetized (cathode) electrode was inserted into the main part of the discharge. Open circuit and resistive load tests were performed to obtain V_o as well as loaded PDC voltages ($V_{\rm PDC}$), current, and power as a function of operating and plasma parameters.

A schematic of the glow discharge tube apparatus is shown in Fig. 1. A gas discharge was initiated in He or Ar at 0.3–3.0 torr between a set of 0.75-in disk discharge electrodes. The discharge anode was welded to a 0.375-in stainless steel (SS) tube to allow concentric access for the PDC anode. The discharge cathode was likewise welded to a 0.375-in SS tube that served both as a vacuum pumping port and electrode. This side of the discharge power delivery was grounded to the experiment platform and power supply ground. The discharge electrodes were separated by 20 cm and are powered by a 600-V, 2-A dc power supply (Xantrex XFR600-2) which produced dc glow plasmas with discharge currents in the range 0.02–150 mA at 300–540 V. Typical discharge operating power for the experiments described here was 10–50 W. A 1-kΩ, 225-W resistor was placed in series with the power supply to limit the discharge current and stabilize the discharge.

The PDC electrodes were fabricated from pure tungsten weld rod of 0.04-in diameter. The collector anode was welded in the shape of a "T" which was then attached to a 12-in-long 1/8-in diameter SS rod that passed through the vacuum seal and provided electrical connection. The PDC cathode was fabricated in a similar fashion absent the T assembly. The T-anode was positioned via a sliding seal and was made continuously rotatable to allow alignment with the axis of the electromagnet. This ensured field line alignment with the surface of the collector electrode. Teflon end caps were fitted to the T-anode ends to preclude electron collection on the butt ends of the anode rod where field lines intersected the collector. The end caps defined the active collection length of the anode as 1.5 cm and the active collection area as 4.79×10^{-5} m^2.

PDC anode magnetization was provided by a 4-in diameter Helmholtz-type electromagnet coil. The coil consisted of 360 turns of 18-gauge magnet wire wound on an aluminum spool. The spool was machined to allow water flow from a chiller at 4 °C–20 °C and 15 L/min through the spool on the inboard side of the windings. The magnet coil was powered by an 80-V, 37-A (Sorensen DCS 80-37) dc power supply. The coil could be indefinitely operated with a steady current of 5 A. The temperature rise measured by an imbedded K-type thermocouple was found to be less than 100 °C under these conditions. Magnetic induction as a function of coil current was measured to be $\sim$67.7 G/A in air. Field uniformity was measured to be $\pm$1.5% at 10 mm from the axis along the center plane of the magnet.

A schematic of the microwave plasma experiment is shown in Fig. 2. This setup comprised a 1.5-kW maximum output power, 2.45-GHz microwave power unit and generator with circulator and dummy load (Applied Science and Technology, ASTEX-AX2100); three-stub tuner (AX3041); and downstream plasma applicator (AX7610). The device was typically operated at 200–1000 W cw with $\leq$1% reflected power. Tap water at $\sim$20 °C and 0.65 L/min was sufficient to cool the applicator to allow continuous operation at full rated power. A mass flow controller (MKS 1179A) provided steady, regulated He gas flow in the range 0–100 sccm. Device performance, however, was not found to be influenced by changes in the mass flow rate. A flow rate of 50 sccm was, therefore, used throughout since this choice proved convenient for pressure adjustment. Throttling the vacuum valve allowed adjustment of the He gas pressure in the range of 0.2–10 torr for the experiments discussed here. A UV light "soft" initiator lamp

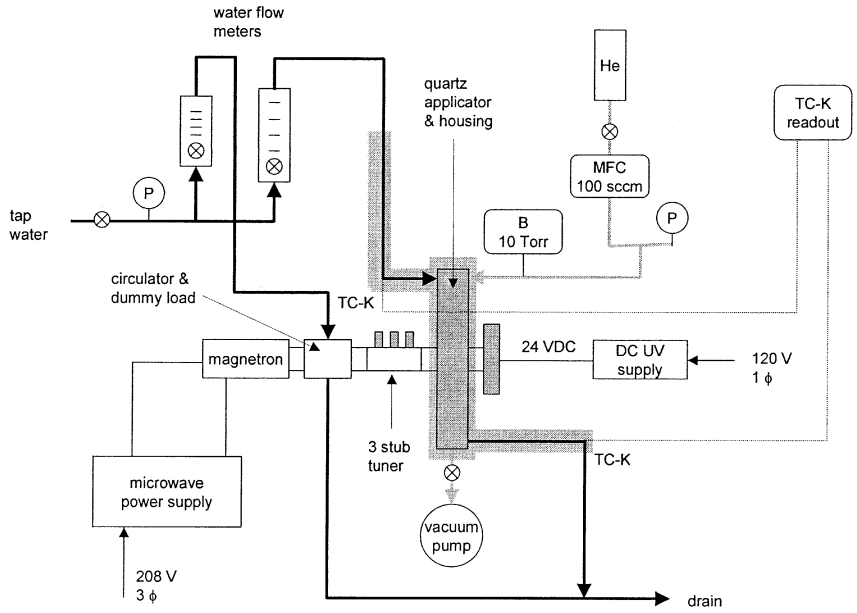

Fig. 2. Schematic of the microwave discharge experiment apparatus. Symbol definitions are as follows: P—pressure gauge; B—Baratron pressure gauge; MFC—mass flow controller; TC-K—type-K thermocouple; DC UV—dc power supply for the UV "soft" initiator. PDC electrodes and magnet coil are not shown.

was provided for breakdown initiation, but was not required in the discharges studied here.

The PDC electrodes employed in the gas discharge cell were replicated for use in the microwave system with the following exceptions: 1) the T-anode was changed to a 0.094-in diameter SS rod to increase the collection area to 1.125×10^{-4} m^2 and 2) the Teflon end caps were replaced with diamond-tool machined hard Alumina as it is well known that only W, SS, and Alumina are able to survive the high-power plasma environment in the microwave system. The same electromagnet set was used in both systems. For the microwave system, the coil separation had to be increased from ∼1.25 in to 3 in resulting in a reduction in the induction calibration to ∼27.9 G/A in air.

A single-tipped Langmuir probe was employed to measure n and T_e in both experiments. The probe consisted of a 0.04-in diameter W weld rod tip extending 5 mm beyond the end of a short section of Alumina 2-bore with 0.052-in ID and 0.156-in OD which was then telescoped inside a 12-in-long section of Alumina single bore, 0.188-in ID and 0.25-in OD. Using a separate 600-V, 2-A dc power supply, the probe was biased over the current–voltage characteristic from full ion saturation to the exponential electron collection region. Probe bias was manually swept from 30–50 V below to several volts above the floating potential. The collisionless, thin-sheath model was employed for probe data analysis such that the probe current was related to the electron density n, electron temperature T_e, sheath thickness x_s, and plasma potential V_p, by

$$i_{\text{probe}} = en\sqrt{\frac{kT_e}{M}}\, A(1 + x_s/r_p) \cdot \left\{ \frac{1}{2}\left(\frac{2M}{\pi m}\right)^{1/2} \exp\left[\frac{e}{kT_e}(V - V_p)\right] - \exp(-1/2) \right\}$$

where A is the probe surface area and r_p is the probe radius. The probe area correction $(1 + x_s/r_p)$ allows for sheath expansion

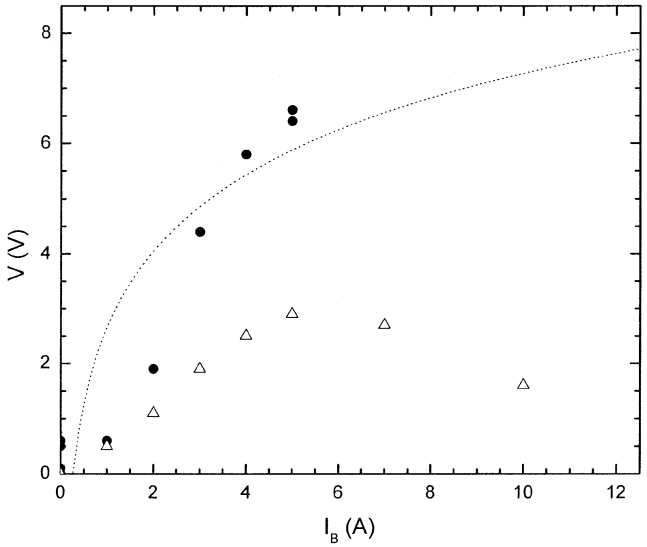

Fig. 3. Open circuit (•) and 20 kΩ PDC (△) voltages in the glow discharge experiment as a function of magnet coil current (67.7 G/A). Nominal operating conditions were 100 mA and 350 V discharge current and voltage. The dotted line shows the predicted open circuit voltage from (4).

with increasing bias potential away from the plasma potential. A nonlinear least squares filter based on the Levenberg–Marquardt algorithm was used to find the four free parameters cited previously. Plasma parameters were found in the range 1–2 eV and 2.5–6.2 $\times 10^{10}$ cm^{-3} in the glow discharge experiment, and 2–6.5 eV and 1–3.2 $\times 10^{12}$ cm^{-3} in the microwave generated plasmas.

IV. Results and Discussion

The results from PDC experiments in the glow discharge device are shown in Figs. 3–7. The nominal operating conditions for the glow discharge tube were ∼100 mA and ∼350 V discharge current and potential, and 1 torr He gas fill. In Fig. 3,

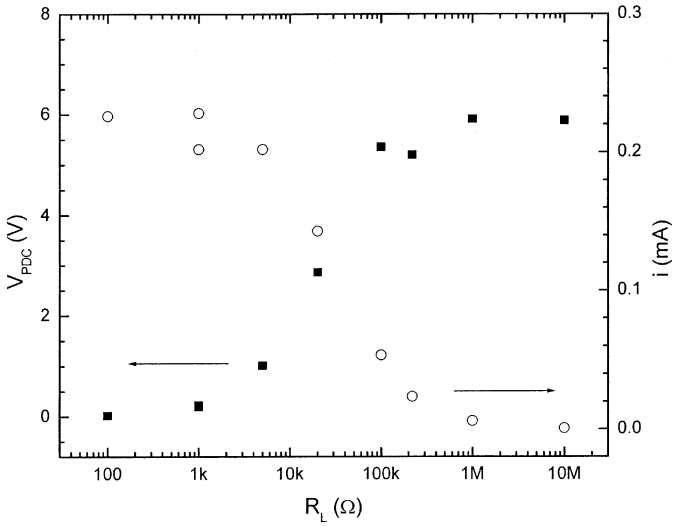

Fig. 4. PDC extracted voltage (■) and current (∘) for load resistances from 100 Ω to 10 MΩ in the glow discharge experiment in 1 torr He and $I_B = 5$ A.

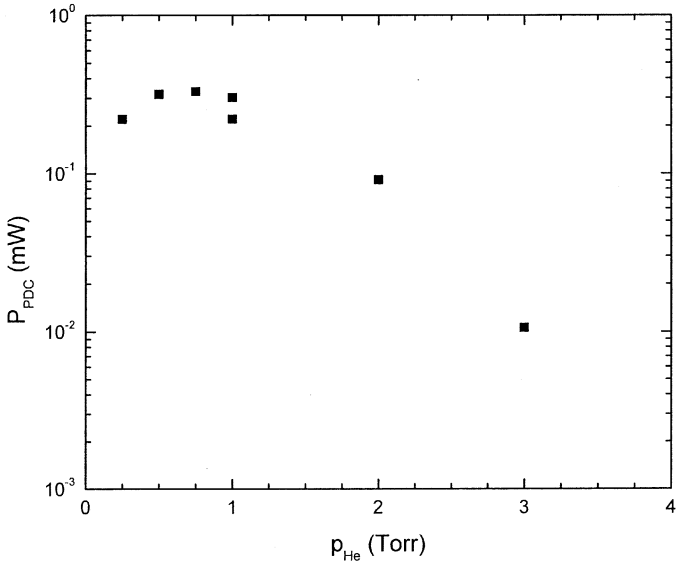

Fig. 6. PDC extracted power as a function of He gas fill pressure in the glow discharge experiment at $R_L = 20$ kΩ and $I_B = 5$ A.

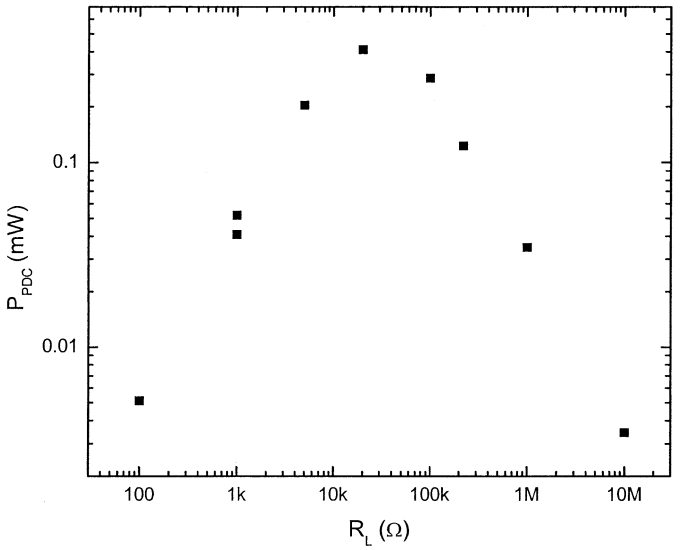

Fig. 5. PDC extracted power as a function of load resistance in the glow-discharge experiment in 1 torr He and $I_B = 5$ A.

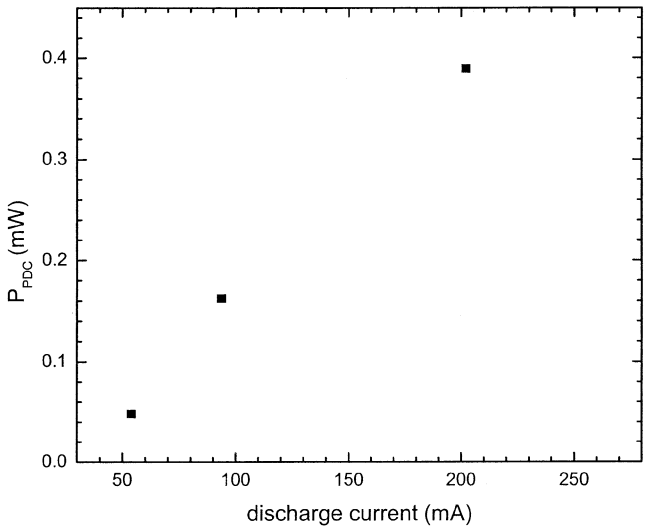

Fig. 7. PDC extracted power as a function of discharge current in the glow discharge experiment at 1 torr He and $I_B = 5$ A.

both open circuit (V_o) and PDC ($V_{\rm PDC}$) voltages are shown as a function of magnet coil current. The evaluation of (4) with $kT_e \sim 1.92$ eV and $\Omega = 18.9$ at $I_B = 5$ A ($B = 350$ G) is also shown for comparison. There is reasonable agreement here with the measured open circuit voltage. The PDC potential with the circuit loaded to 20 kΩ is also shown in Fig. 3. The loaded PDC voltage was found to be consistently $\sim 1/2 V_o$ indicating that this load impedance was close to that of the PDC source for the conditions of this experiment.

Figs. 4 and 5 summarize the PDC results obtained by varying the load resistance from 100 Ω to 10 MΩ. In Fig. 4, the PDC voltage was observed to increase steadily from the short circuit condition at $R_L \lesssim 1$ kΩ to voltages approaching the open circuit voltage (>6 V) at $R_L \gtrsim 1$ MΩ. The PDC current decrease was found to be consistent with the output voltage trend. The PDC extracted power to load R_L is shown in Fig. 5 as a function of load resistance (power–load curve). The power–load curve peaks at the impedance matched condition ∼20 kΩ at a maximum extracted power of ∼0.44 mW.

The results of varying the helium fill pressure and discharge current as potential routes to increase the extracted power are shown in Figs. 6 and 7, respectively. At the load matched condition $R_L = R$ the peak extracted PDC power should be expected to behave as $(V_o)^2/R$. At constant B, ignoring the weak logarithmic dependence in the other contributors to Ω, and considering only electron–neutral collisions, the PDC power scaling predicts

$$P_{\rm PDC} \sim \frac{n}{n_n} T_e^{3/2} \tag{6}$$

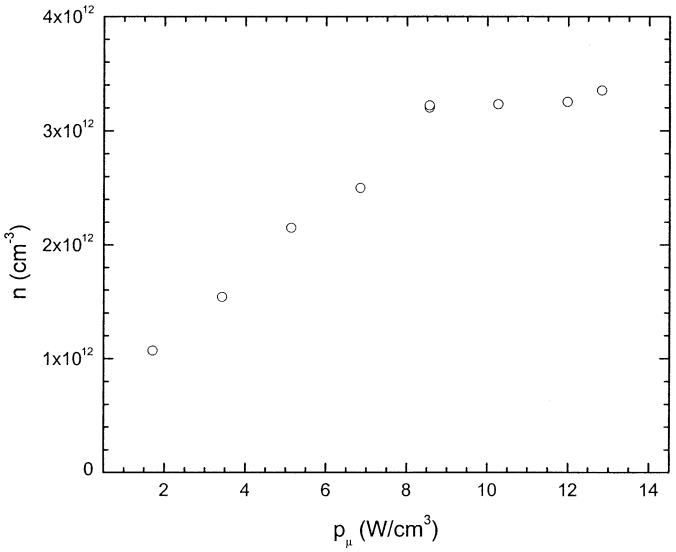

Fig. 8. Langmuir probe measurements of electron density in the microwave experiment as a function of microwave power density for 1 torr He at 50 sccm.

TABLE I
DEVICE AND DISCHARGE CONDITIONS FOR 1 torr He

Parameter	Glow Discharge Experiment	Microwave Experiment
A_p (m^2)	4.79×10^{-5}	1.125×10^{-4}
V_{PDC} (V)	6.5	7.5
n (cm^{-3})	5×10^{10}	3×10^{12}
n_n (cm^{-3})	3×10^{16}	3×10^{16}
T_e (eV)	1.5	3.7
Ω	18.9	4.8

where n_n is the neutral atom density in the discharge tube which is proportional to the gas fill pressure. Holding T_e constant, $P_{\rm PDC}$ can be expected to scale as

$$P_{\rm PDC} \sim \frac{i_{\rm discharge}}{P_{\rm He}} \tag{7}$$

where $i_{\rm discharge}$ is the glow-discharge current and $p_{\rm He}$ is the He gas pressure. $P_{\rm PDC}$ increased with increasing glow discharge current and decreasing He gas pressure according to (7) as shown in Figs. 6 and 7.

The observed PDC power scaling with discharge current and pressure in the discharge device suggests obvious paths to power scale-up through reduction in the neutral to charge density ratio and concomitant increase in the plasma conductivity. At similar He fill pressure (i.e., $\sim$1 torr), the microwave device operated at greatly increased charge density over that in the glow discharge experiment. Fig. 8 shows the results of Langmuir probe electron density measurements in the microwave experiment at 1 torr He as a function of microwave power density. The result was a density scale-up by almost two orders in magnitude over the glow experiment results.

Device and discharge conditions were compared for the two experiments in Table I. A direct application of (4) predicted an open circuit voltage scale up by $\sim$33% in the microwave experiment. Fig. 9 shows $V_{\rm PDC}$ and i as functions of load resistance for 1 torr He microwave plasma at 8.55 W/cm^3 input power density. The asymptote in $V_{\rm PDC}$ is the open circuit voltage approaching 7.5 V, an increase of $\sim$15.4% over that in the discharge experiment.

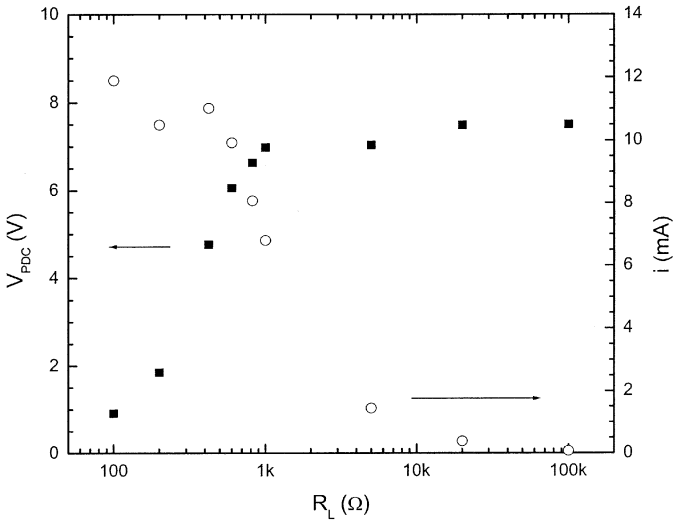

Fig. 9. PDC voltage (■) and current (∘) as a function of load resistance in the microwave device at 8.55 W/cm^3, and 1 torr He at 50 sccm.

An estimate of the PDC power scale-up across two experiments is given by combining the predicted potential scaling [(4)] with expected conductivity change based on electron–neutral collisions such that

$$\frac{P_{\rm PDC_2}}{P_{\rm PDC_1}} = \frac{V_{\rm PDC_2}}{V_{\rm PDC_1}}\frac{i_2}{i_1} = \left(\frac{V_{0_2}}{V_{0_1}}\right)^2 \frac{R_1}{R_2} = \left(\frac{kT_{e_2}}{kT_{e_1}}\right)^{3/2} \left[\frac{\ln(1+\Omega_2^2)}{\ln(1+\Omega_1^2)}\right]^2 \frac{(A_p n)_2}{(A_p n)_1}\frac{n_{n_1}}{n_{n_2}} \tag{8}$$

where subscripts 1 and 2 refer to differing devices or conditions, and A_p is the PDC electrode active collection area. Comparing the microwave device conditions with those in the glow discharge for the potential ratio found previously and the device parameters found for 1 torr He discharges in the respective devices enumerated in Table I, a PDC power scale-up factor of 158.4 was predicted.

PDC extracted power is shown in Fig. 10 as a function of R_L for the microwave discharge conditions of Table I. The optimal (impedance matched) condition in this case was near 600 Ω where the peak PDC power was 60 mW, a factor of 136.4 over that obtained in the glow discharge experiment.

Further improvement has been identified by varying the operating conditions slightly to 0.75 torr He at 50 sccm. Figs. 11 and 12 show $V_{\rm PDC}$ and $P_{\rm PDC}$, respectively, as functions of the microwave power density for this pressure and 600 Ω load. This case demonstrated the maximum observed PDC performance. The PDC power increase to $\sim$220 mW was consistent with a measured T_e increase to $\sim$7 eV over the 1 torr case [(4)]. Plasma density measured for this enhanced PDC performance case was similar to the 1 torr case (Fig. 8). The asymptotic behavior in the PDC power with microwave power shown in Fig. 12 is consistent with the leveling off of the plasma conductivity suggested by the density roll-over in Fig. 8.

The conversion efficiency, ε, is estimated as the ratio of conversion to input power densities in the plasma discharge device

$$\varepsilon = \frac{p_{\rm PDC}}{p}. \tag{9}$$

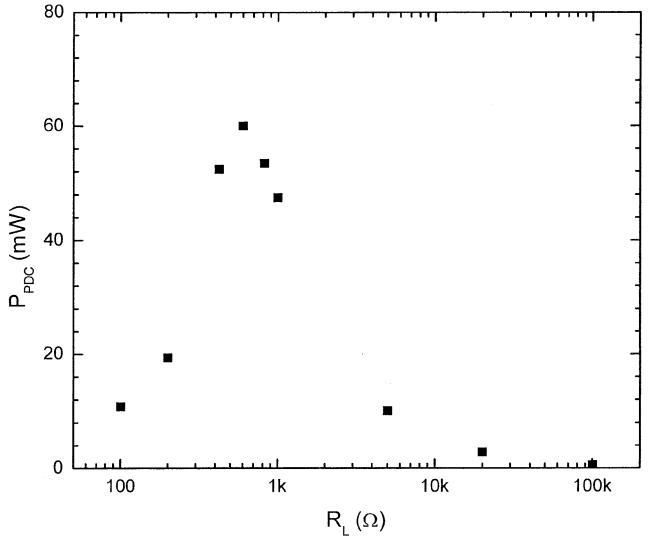

Fig. 10. PDC extracted power as a function of load resistance in the microwave device at 8.55 W/cm^3, and 1 torr He at 50 sccm.

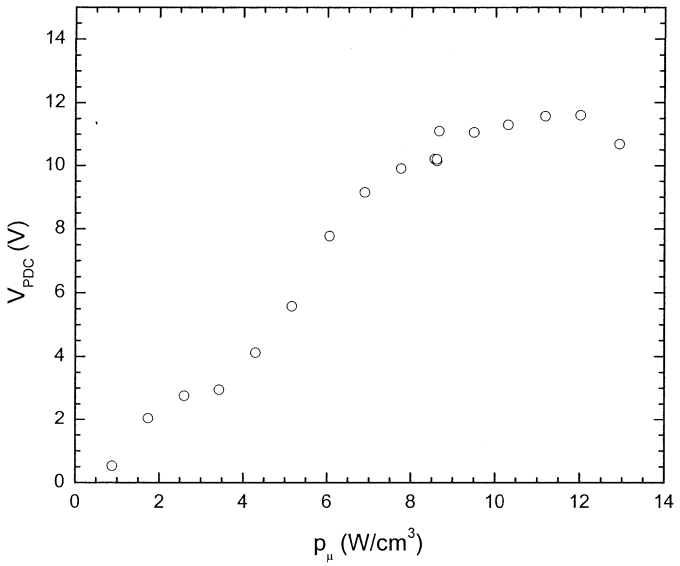

Fig. 11. PDC potential as a function of microwave power density for $R_L = 600\ \Omega$, and 0.75 torr He at 50 sccm.

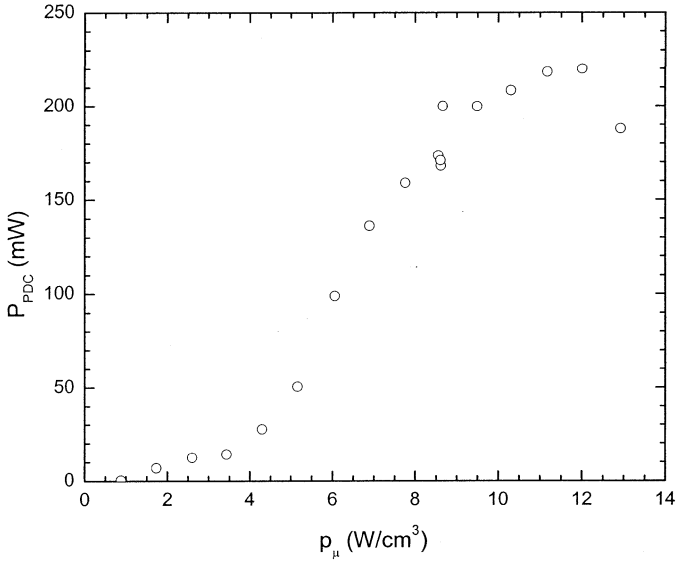

Fig. 12. PDC extracted power as a function of microwave power density for $R_L = 600\ \Omega$, and 0.75 torr He at 50 sccm.

Here, $p_{\rm PDC} = P_{\rm PDC}/V_{\rm PDC}$, where $V_{\rm PDC}$ represents the plasma volume accessible to PDC power extraction, and p is the input power density to generate and sustain the discharge. (In a CA plasma, the external power input may be reduced substantially below that required in a non-CA plasma.) As the probe's electrostatic influence does not extend beyond the presheath, the relevant interaction volume is defined by the electron mean-free path for collisions in this high pressure discharge, and becomes an annular cylindrical volume surrounding the probe extending λ_{mfp} from the probe surface. By way of example for the microwave discharge experiment, at 1 torr in He the electron $\lambda_{mfp} \sim 0.082$ cm. The PDC accessible plasma volume is then $\sim$0.124 cm^3, making the collection power density $\sim$1.61 W/cm^3 and the conversion efficiency $\sim$18.8% for this case.

The V_o scaling with electron temperature [(4)] indicates a strong T_e dependence in the conversion efficiency, [(9)]. Furthermore, the inverse dependence on plasma resistance ($\varepsilon \sim 1/R = A_p/\eta l$) reflects positive probe area scaling and inverse plasma resistivity scaling, indicating clear directions for further performance improvement. Further optimization of PDC power conversion on a single electrode set is in progress as well as power scale-up with multiple electrode sets. A linear power scale-up is anticipated. It is, however, recognized that indefinite increase in electrode number and size relative to that of the discharge is not possible without interfering with plasma conditions. A more detailed efficiency analysis incorporating the affect of electrode perturbation on the plasma should be considered. Discharge seeding by CA-plasma catalysts such as certain alkali and alkali–earth metals [11] to increase charge density may also be employed in an effort to increase conductivity, extracted power, and efficiency, and may also lead to increases in the CA-plasma power.

V. Conclusion

Standard glow-discharge and microwave-plasma generation sources that provide reproducible, stable plasmas with power densities on the order of those of CA-plasmas were used to characterize plasmadynamic power conversion. The PDC generation of electrical power was experimentally demonstrated at the $\sim$1/4 W level in laboratory plasma devices for the first time. Glow discharge and microwave plasma sources were operated at power levels up to 50 W and 11.97 W/cm^3, respectively. In a glow discharge of 1 torr He fill with $T_e \sim 1.9$ eV and $n \sim 2.8 \times 10^{10}$ cm^{-3}, PDC open circuit voltages were shown to increase with applied field strength (0–350 G) up to 6.5 V. These results were demonstrated to be in reasonable agreement with a simple model describing electron current retardation to a magnetized electrode. Power–load curves identify the impedance matching condition at 20 kΩ, for which the peak PDC extracted power is 0.44 mW.

Electron and neutral particle density scaling experiments for $P_{\rm PDC}$ reveal the strong dependence on plasma conductivity. Power scale-up was demonstrated in a microwave device which

generated plasmas in 1 torr He with $T_e \sim 3.7$ eV and $n \sim 3.2 \times 10^{12}$ cm^{-3}. The charge density, electron temperature, and electrode collection area scale-up were the dominant affects in a PDC power scale-up by a factor of almost 140 over the glow-discharge PDC results. PDC extracted power to 60 mW was found in a 1 torr He microwave discharge at 8.55 W/cm^3 and 600 Ω load match. The reduced load match was itself evidence of a greatly enhanced plasma conductivity. $P_{\rm PDC}$ to $\sim$200 mW was found in the microwave experiment at 8.55 W/cm^3 and 0.75 torr He. Peak output performance to 220 mW PDC power was obtained at 11.97 W/cm^3 microwave input.

Plasmadynamic conversion may be optimized for high power and efficiency. The system is simple with projected costs on the order of 1% those of fuel cells. The implications for microdistributed power are profound. Scale-up to several to 10 s of W in a small, modular array converter unit is under development. Autonomous, chemically driven, power producing plasma units outfitted with plasmadynamic collection devices are envisioned which could enable microdistributed electrical and motive power applications without infrastructure requirements other than those of its manufacture and distribution.

ACKNOWLEDGMENT

The authors would like to thank Dr. M. Nansteel for many useful discussions and excellent technical assistance during the experimental phase of this effort.

REFERENCES

[1] R. G. Mills, "Some engineering problems of thermonuclear reactors," *Nucl. Fusion*, vol. 7, pp. 223–236, 1967.
[2] D. L. Rose, "Engineering feasibility of controlled fusion," *Nucl. Fusion*, vol. 9, pp. 183–203, 1969.
[3] G. H. Miley, *Fusion Energy Conversion*. La Grange, IL: Amer. Nucl. Soc., 1976.
[4] R. L. Mills, N. Greenig, and S. Hicks, "Optically measured power balances of glow discharges of mixtures of argon, hydrogen, potassium, rubidium, cesium, or strontium vapor," *Int. J. Hydrogen Energy*, vol. 27, pp. 651–670, 2002.
[5] R. Mills, M. Nansteel, and Y. Lu, "Observation of extreme ultraviolet hydrogen emission from incandescently heated hydrogen gas with strontium that produced an anomalous optically measured power balance," *Int. J. Hydrogen Energy*, vol. 26, no. 4, pp. 309–326, 2001.
[6] R. L. Mills and P. Ray, "Substantial changes in the characteristics of a microwave plasma due to combining argon and hydrogen," *New J. Phys.*, vol. 4, pp. 22.1–22.17, 2002. [Online]. Available: www.njp.org.
[7] R. M. Mayo, R. L. Mills, and M. Nansteel, "On the potential for direct or MHD conversion of power from a novel plasma source to electricity for microdistributed power applications," *IEEE Trans. Plasma Sci.*, to be published.
[8] I. Alexeff and D. W. Jones, "Collisionless ion-wave propagation and the determination of the compression coefficient of plasma electrons," *Phys. Rev. Lett.*, vol. 15, pp. 286–288, 1965.
[9] F. F. Chen, "Electric probes," in *Plasma Diagnostic Techniques*, R. H. Huddlestone and S. L. Leonard, Eds. New York: Academic , 1965.
[10] D. Bradley, S. M. A. Ibrahim, and C. G. W. Sheppard, *Fourteenth Symposium (International) on Combustion*. Pittsburgh, PA: Combustion Inst., 1973, p. 383.
[11] R. Mills, J. Dong, and Y. Lu, "Observation of extreme ultraviolet hydrogen emission from incandescently heated hydrogen gas with certain catalysts," *Int. J. Hydrogen Energy*, vol. 25, pp. 919–943, 2000.

Robert M. Mayo (M'91) received the Ph.D. degree in nuclear engineering from Purdue University, West Lafayette, IN, in 1989.

He is currently the Director of the Plasma-to-Electric Conversion Program at BlackLight Power (BLP), Inc., Cranbury, NJ. He served most recently on the faculty in the Department of Nuclear Engineering, North Carolina State University, Raleigh, where, among other responsibilities, he served as Director of Graduate Programs. His research interests include pulsed laser evaporated (PLE) plasmas for advanced materials production, imaging, spectroscopic and particle plasma diagnostics for thin-film heterostructures using pulsed laser deposition, and magnetized PLE plasma for plume control and controlled deposition. At BLP, he provides expertise in the detailed characterization of chemically-driven plasma, as well as leadership in the analysis, design, and development of a plasma–to-electric conversion prototype. He has published a book *Introduction to Nuclear Concepts for Engineers* (LaGrange Park, IL: ANS, 1998), 40 journal articles, and has presented in more than 70 conferences.

Dr. Mayo is a member of the American Physical Society-Division of Plasma Physics, and the American Nuclear Society.

Randell L. Mills received the B.A. degree in chemistry (*summa cum laude* and Phi Beta Kappa) from Franklin & Marshall College, Lancaster, PA, and the M.D. degree with a concentration on technology from Harvard Medical School, Cambridge, MA, in 1982 and 1986, respectively. He also studied electrical engineering at the Massachusetts Institute of Technology, Cambridge.

He is the Founder and President of BlackLight Power, Inc., Cranbury, NJ, a company that is developing technologies based on novel hydrogen chemistry. He has authored or co-authored over 85 articles and a book in this field. He is also active in a number of other areas of technology. He has received or filed patent applications in magnetic resonance imaging, Mossbauer cancer therapy, Luminide class of drug delivery molecules, genomic sequencing method, and artificial intelligence.

Dr. Mills is a member of the American Chemical Society.